International Journal of Mechanical, Industrial and Aerospace Sciences
ISSN: 2517-9950
Vol:11, No:11, 2017

Effect of Non-Newtonian Behavior of Oil Phase on Oil-Water Stratified Flow in a Horizontal Channel

Satish Kumar Dewangan, Santosh Kumar Senapati

Abstract**—**The present work focuses on the investigation of the effect of non-Newtonian behavior on the oil-water stratified flow in a horizontal channel using ANSYS Fluent. Coupled level set and volume of fluid (CLSVOF) has been used to capture the evolving interface assuming unsteady, coaxial flow with constant fluid properties. The diametric variation of oil volume fraction, mixture velocity, total pressure and pressure gradient has been studied. Non-Newtonian behavior of oil has been represented by the power law model in order to investigate the effect of flow behavior index. Stratified flow pattern tends to assume dispersed flow pattern with the change in the behavior of oil to non-Newtonian. The pressure gradient is found to be very much sensitive to the flow behavior index. The findings could be useful in designing the transportation pipe line in petroleum industries.

Keywords**—**Oil-water stratified flow, horizontal channel, CLSVOF, non –Newtonian behavior.

I. Introduction

THE present work investigates the stratified flow pattern. Stratified flows are important in many practical applications such as in the transportation pipeline of petroleum industry, heat exchangers, thermal storage tanks, geothermal industry, nuclear industry, chemical industry, process industry etc. Stratified flow is characterized by the presence of clear interface between the phases present in the flow. The interface may be smooth, wavy or may also have slight dispersion of one phase into other.

Several researchers have analyzed stratified flow patterns. Elseth [3] has studied the behavior of simultaneous flow of oil and Water in horizontal pipes considering the effect of mixture velocity and inlet water cutoff on flow pattern transition was studied. Pandey et al. [8] investigated the liquid-liquid two phase flows in a horizontal pipe and reported that higher water velocities have small effect on stratified flow. Rodriguez and Baldani [9] have studied the effect of superficial velocities of oil, water and inclination angles on the pressure gradient and hold up in oil-water stratified flow. Goldstein et al. [7] have presented analytical expressions for velocity profile, pressure gradient and shear stress in laminar stratified flow for both concave and convex interfaces in horizontal and inclined flow systems. Gada and Sharma [4], [5] presented analytical solution for fully developed two phase stratified flow in an inclined channel. Das et al. [1] used level set method to investigate the effect of viscosity ratio on the laminar two phase stratified flow pattern in a circular cross-section pipe. Rodriguez and Baldani [9] have obtained the pressure gradient for oil-water stratified flow using CFD. Gada et al. [2] studied the two phase stratified flow with and without phase change in a plane channel subjected to different thermal boundary conditions.

From a careful survey of available literature, it is concluded application of the CLSVOF method for the simulation of oil-water stratified flow is found to be rare. The aspect of stratified flow such as effect of non-Newtonian behavior of fluid, temperature analysis using CLSVOF has been paid very little attention. Thus, in this work, attempt has been made to investigate the stratified flow phenomena using CLSVOF to capture the interface. The non-Newtonian cases that have been simulated in this work are listed in Table I.

TABLE I
DETAILS OF CASES SIMULATED FOR PREDICTION OF THE EFFECT OF NON-NEWTONIAN BEHAVIOR ON STRATIFIED FLOW

S. N.	*K* (Flow consistency index)	*n* (Flow behavior index)
1	2.5042	0.9573
2	2.5042	0.8546
3	2.5042	0.7522

II. Mathematical Modeling

The CLSVOF method utilizes advantages of both Piece wise linear interpolation scheme VOF (Volume of Fluid) and LSM. In CLSVOF, the interface is represented by volume fraction function so that mass is conserved while still maintaining a sharp representation of the interface.

A. Volume of Fluid Method

This method uses a volume fraction function (*r*) to indicate what fraction of the total cell volume is occupied by a particular fluid. In each control volume, the sum total of volume fractions of all phases is unity. Hence *r* is 0 or 1 indicates pure fluid cell whereas $0 < r < 1$ in two phase cells.

$$\frac{\partial \rho}{\partial t} + \nabla.(\rho V) = 0 \quad (1)$$

$$\frac{\partial (\rho V)}{\partial t} + \nabla.(\rho VV) = \nabla\tau - \nabla p + B \quad (2)$$

The density and the viscosity are evaluated as:

$$\rho = \sum_{k=1}^{n} r^{(k)} \rho^{(k)} \quad (3)$$

Dr. Satish Kumar Dewangan is Assistant Professor in Mechanical Engineering Department, National Institute of Technology, Raipur (CG) 492010, India (Corresponding Author; phone: (+91) – 94060-75050; e-mail: skdewangan.amech@nitrr.ac.in).

Santosh Kumar Senapati has been M.Tech. (Thermal) scholar in Mechanical Engineering Department, National Institute of Technology, Raipur (CG) 492010, (phone: (+91) – 82804-71656, e-mail: senapatis431@gmail.com).

$$\mu = \sum_{k=1}^{n} r^{(k)} \mu^{(k)} \quad (4)$$

where n is the number of fluid and r^k is the volume fraction of k^{th} fluid. The volume fraction advection equation is given as:

$$\frac{\partial(\rho r^k)}{\partial t} + V.\nabla r^k = 0, for\ k = 1, 2, 3 \ldots\ldots, (n-1) \quad (5)$$

$$\sum_{k=1}^{n} r^{(k)} = 1, for\ k = 1, 2, 3 \ldots\ldots, (n-1) \quad (6)$$

B. Level Set Method

The level set method uses three functions namely: The level set function, the Heaviside function or unit step function and the Dirac delta function. The level set function describes interface as described above in this article; the Heaviside function itself is a function of level set function and is used for calculating the mean fluid properties required at the interface; and the Dirac delta function is used for taking into account the effect of surface tension or interfacial mass transfer etc. into the modeling. Gada and Sharma [6] derived the governing equations and described the physical significance of the terms used in Level set method.

The Heaviside function is defined as

$$H(\phi) = \begin{cases} 0 & if\ \phi < \epsilon \\ \frac{\phi+\epsilon}{2\epsilon} + \frac{1}{2\pi} sin(\frac{\phi\pi}{\epsilon}) & if\ |\phi| \le \epsilon \\ 1 & if\ \phi > \epsilon \end{cases} \quad (7)$$

The Dirac delta function is defined as

$$\delta(\phi) = \begin{cases} \frac{1}{2\epsilon} + \frac{1}{2\epsilon} cos(\frac{\phi\pi}{\epsilon}) & if\ \phi = 0 \\ 0 & otherwise \end{cases} \quad (8)$$

The law of conservation of mass, level set advection equation, momentum equation, energy equation and re-initialization equation are described in (9)-(13) respectively.

$$\nabla.\vec{u} = (\frac{1}{\rho_2} - \frac{1}{\rho_1})\ \dot{m}\frac{\Delta Si}{\Delta V} = \left(\frac{1}{\rho_2} - \frac{1}{\rho_1}\right)\dot{m}\,\delta(\phi) \quad (9)$$

$$\frac{\partial\phi}{\partial t} + \vec{u}_t.\nabla\phi = 0 \quad (10)$$

$$\frac{\partial(\rho_m\vec{u})}{\partial t} + \nabla.(\rho_m\vec{u}\ \vec{u}) = -\nabla P + \nabla.\mu_m(\nabla.\vec{u} + \nabla.\vec{u}^T) + \sigma k\hat{n}\,\delta(\phi) + \vec{B} \quad (11)$$

$$\frac{\partial T}{\partial t} + \nabla.(\vec{u}\,T) = \alpha N\nabla^2 T \quad (12)$$

$$\frac{\partial\phi}{\partial t_s} + S_\epsilon(\phi_0)(|\nabla\phi| - 1) = 0 \quad (13)$$

where t_s is the pseudo time, $S_\epsilon(\phi_0) = \frac{\phi_0}{\sqrt{{\phi_0}^2 + \epsilon^2}}$ is the smoothed sign function.

III. Numerical Formulation

In the present case, for the analysis of oil-water two phases stratified flow, a two dimensional rectangular domain has been chosen. The geometry and detailed dimensions of the domain is shown in Fig. 1. The test section is located at a height of 6.55 m from the origin of the coordinate system.

Water and oil enter into the test section from different inlets through a T-junction. Water enters from horizontal direction and oil from vertical direction. The entire domain [Fig. 1] has been divided into four sections namely: Water inlet boundary, oil inlet boundary, outlet boundary and the test section. This is shown in Fig. 1.

The entire domain was divided into quadrilateral cells to capture surface tension effect more accurately. Mesh independent study was done and mesh with 56502 cells was selected as the optimum mesh.

TABLE II
Details of Properties of Fluid Used in the Simulation

Fluid property	Oil	Water
Density, ρ (kg/m^3)	888.398	998.200
Viscosity, μ (Kg/ms)	0.107321	0.001003
Thermal conductivity, k (W/mK)	0.0944	0.6019
Specific heat, C_p (J/KgK)	1897.214	4156
Surface tension, σ (N/m)	0.024	0.024
Contact angle, α (degree)	8.5	8.5

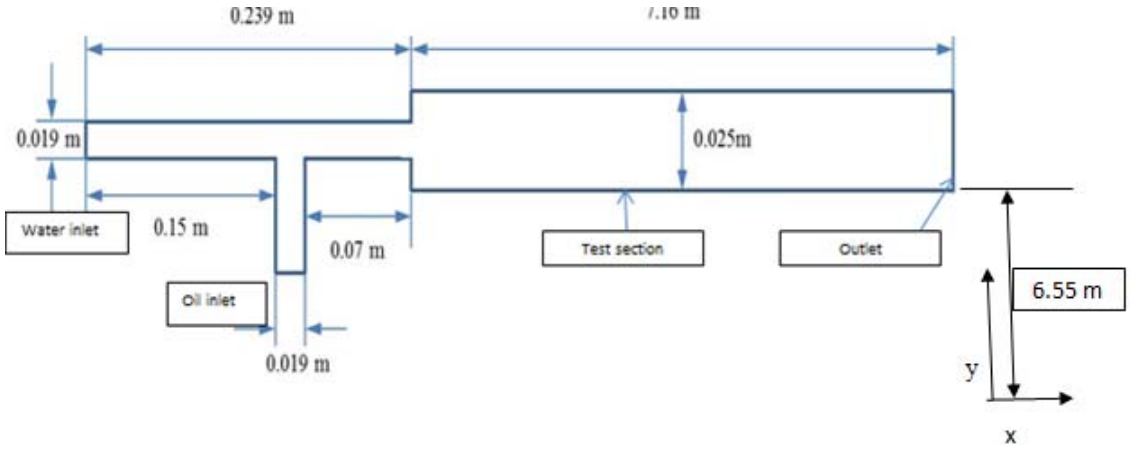

Fig. 1 Schematic representation of domain with detailed dimensions

Fig. 2 Meshing of channel

TABLE II
DETAILS OF BOUNDARY CONDITIONS

Oil inlet	Specified superficial velocity of oil, phase-2 volume fraction = 0, oil temperature at inlet.
Water	Specified superficial velocity of oil, phase-2 volume fraction = 1, water temperature at inlet.
Wall	Stationary wall with no slip boundary condition, contact angle, wall temperature.
outlet	Pressure outlet with zero gauge pressure.

A. Procedure

For all cases first of all the channel has been filled with water from water inlet and then oil has been introduced into it. The steps followed during the simulation are described below.

a. 2D pressure based solver with absolute velocity formulation is chosen as the solver under transient condition. Gravity is considered in the Y-direction as -9.81 m/s^2 and atmospheric pressure is set as operating pressure.
b. CLSVOF is selected with two Eulerian phases. Oil is set as primary phase and water as secondary phase. Surface tension is taken into account using surface tension force modeling.
c. The fluids oil and water are chosen from fluent database and the properties are set to desired value depending up on the case as mentioned in Table II. For predicting the effect of non-Newtonian behavior power, law model is selected for oil.
d. After this, the flow and thermal boundary conditions for the simulation of the various cases are applied.
e. PISO scheme is used for pressure velocity coupling. PRESTO is used for pressure discretization. Volume fraction is discretized using geo-reconstruct. Power law scheme is used for momentum and level set function. First order implicit is used for the transient formulation .Under-relaxation parameters are retained at default values. Residue value is set at 10^{-04}.
f. Variable time stepping method with iterative time stepping is used. Courant number is always kept below 1. The results are taken when steady state is achieved.

B. Mesh Refinement Study and Validation

Fig. 3 shows the variation of oil volume fraction with radial distance for all the five meshes. From Fig. 3, it is observed that there is significant variation of oil volume fraction when the mesh is refined from 27953 cells to 35830 cells. However, the variation oil volume fraction for meshes with 48152 cells, 56502 cells and 69570 cells are almost identical. More particularly the results of fourth (56502 cells) and fifth mesh (69570 cells) are almost overlapping. Thus, the fifth mesh with 56502 numbers of cells has been selected as the optimum mesh for simulation

The FLUENT procedure for the case has been validated with the experimental results of Elseth [3].

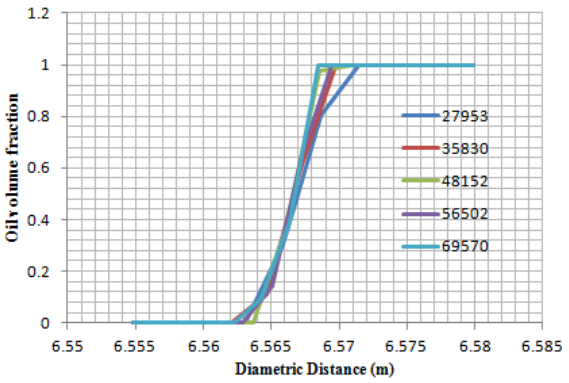

Fig. 3 Diametric variation oil volume fraction for different mesh size

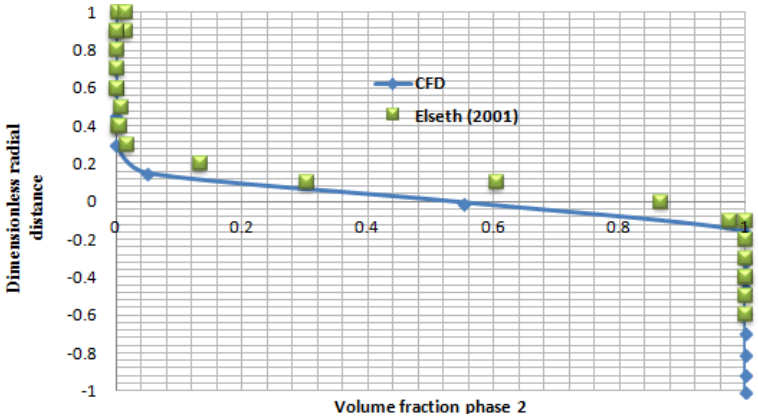

Fig. 4 Comparison of water volume fraction profile with Elseth [3]

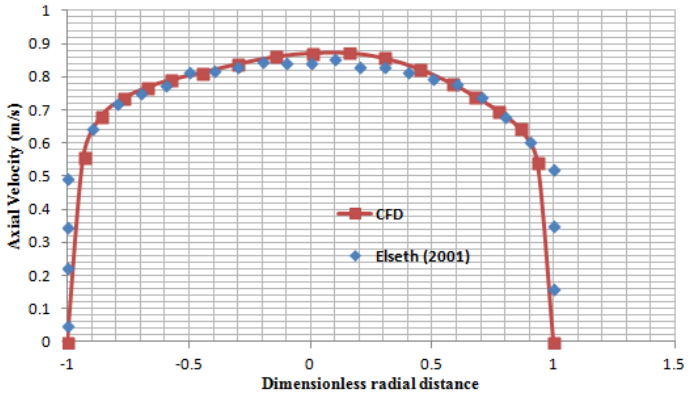

Fig. 5 Comparison of axial velocity profile with Elseth [3]

Out of several experimental cases of Elseth [3], one case was chosen for the validation purpose in which the mixture velocity at the inlet is 0.67 m/s and the inlet water cut (volume fraction) is 0.5. The diameter of the pipe is 0.05575 m and the length of the test section is chosen as 5 m so that fully developed condition is attained within the pipe length. For validation purpose, the same geometry and dimensions of the domain as well as the fluid properties have been used as Elseth [3]. However, instead of pipe, a two dimensional channel has been chosen to reduce the computational time and cost. *k-ω* turbulence model has been used. The relaxation parameters used during the simulation is given in Table IV. The volume fraction profile of water and the velocity profile have been compared with the experimental results and an excellent agreement is obtained between the experimental work and the CFD even for two dimensional domain as shown in Figs. 4 and 5 respectively. Thus, the computational procedure is found to be a good one and hence the same procedure has been used throughout the simulation.

TABLE IV
DETAILS OF UNDER-RELAXATION PARAMETERS

Variables for under-relaxation parameter	Parameter value
Pressure	0.3
Density	1
Body forces	1
Momentum	0.4
Level set function	0.3

IV. RESULTS AND DISCUSSION

It is interesting to note that the oil in oil wells can behave as Newtonian and non-Newtonian fluid depending on the strain rate and morphological parameters of the fluid. Thus it is essential to investigate the effect of non-Newtonian behavior of oil on stratified flow pattern and to predict the changes taking place as compared to the case when both fluids behave as Newtonian. In this section, effort has been made to investigate the non-Newtonian behavior of oil on volume fraction profile, mixture velocity profile, total pressure of mixture and pressure drop. The oil is assumed to follow the power law model. The flow consistency index is kept constant and the flow behavior index is varied to observe its effect on the flow pattern keeping all other parameters same as that of the previous case. The superficial phase velocities of oil and water are 0.2 m/s and 0.23 m/s respectively. The details are shown in Table V.

TABLE V
DETAILS OF POWER LAW MODEL USED FOR OIL

S. N.	K (Flow consistency index)	n (Flow behavior index)
1	2.5042	0.7522
2	2.5042	0.8546
3	2.5042	0.9573

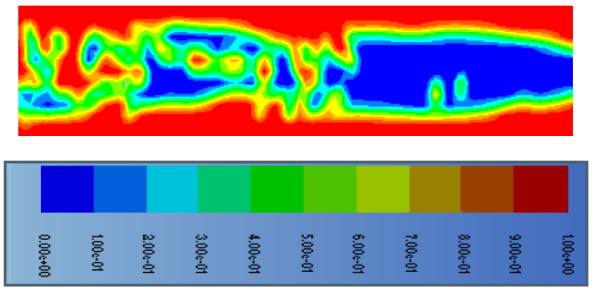

(a)

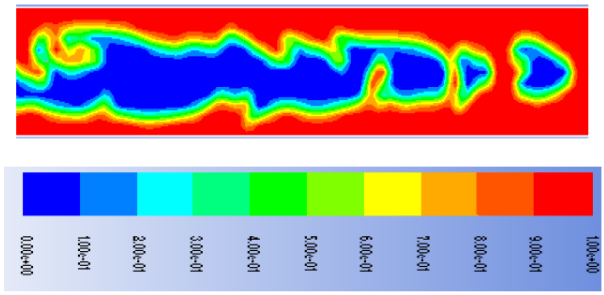

(b)

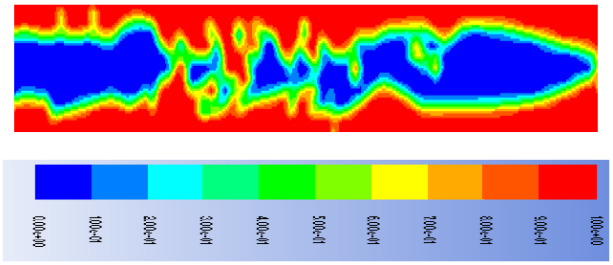

(c)

Fig. 6 Contours of oil (phase1) volume fraction for (a) n=0.7522 (b) n=0.8546 (c) n=0.9573

The contours of oil volume fraction are shown in figure 6. It is interesting to note that as the behavior of oil is changed from Newtonian to non-Newtonian keeping other parameter constant entire flow pattern is changed from stratified to disperse throughout the length of pipe. A change in flow pattern affects the pressure drop severely. This is discussed below.

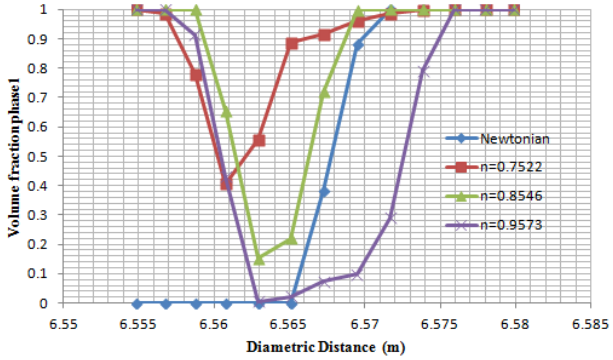

Fig. 7 Diametric distribution of oil volume fraction at different flow behavior index

Fig. 7 shows the diametric variation of volume fraction at different flow behavior index. As it is seen from the figure that due to disperse flow, the volume fraction profile does not have any particular trend. However it can be seen from the graph that the near wall region is mostly occupied by oil phase as the graph depicts volume fraction value of 1 in this region for all the three sub cases. Dispersion mainly takes place in a region near the center portion of the channel. Amount of oil phase located on the top portion of channel is observed to be maximum for n = 0.8546 followed by n = 0.9573 and n = 0.7522. Similarly dispersion starts at a higher radial distance from the bottom of the channel for n = 0.8546. For n = 0.7522 and 0.9573 dispersion starts at a radial distance slightly ahead as compared to n = 0.7522. The diffusion is found to be more for flow behavior index of 0.9573. The steepness of the volume fraction curves increases with increase in flow behavior index. Also the volume fraction curves are more open at higher value of flow behavior index.

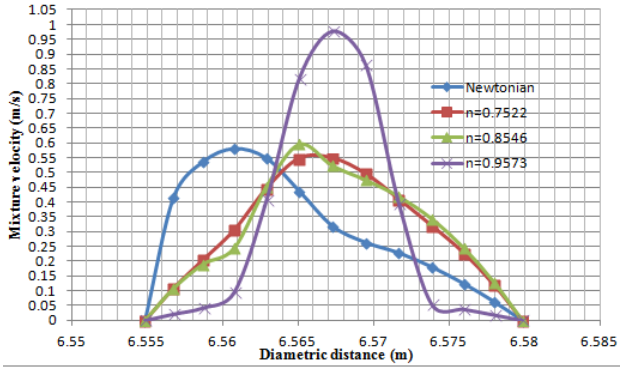

Fig. 8 Diametric distribution of mixture velocity at different flow behavior index

Fig. 8 shows the diametric variation of mixture velocity at different flow behavior index. As it is seen from the figure, there is a considerable variation in mixture velocity when non-Newtonian behavior is considered. For n = 0.7522 and 0.8546 the velocity profiles are almost similar whereas for n = 0.9573 a completely different velocity profile is observed. For the former cases, the velocity variations are found to be gradual whereas for n = 0.9573, the velocity profile is found to be steep. Higher velocities are observed nearly at the center region of pipe where the dispersion takes place. A huge change in the maximum value of velocity is not noticed among the cases: Newtonian fluids, n=0.7522 and n = 0.8546 and found to lie in the range of 0.55m/s to 0.65 m/s. However the maximum velocity for the case n = 0.9573 is found to be almost 0.98 m/s. Also it is observed that the maximum velocity for the non-Newtonian cases is obtained at a higher diametric location as compared to the case where both fluids are Newtonian.

The diametric variation of total pressure of mixture at different flow behavior index is shown in Fig. 9. Graph shows that the total pressure of mixture is severely affected by the variation in the flow behavior index.

There is a huge difference in the diametric total pressure distribution when oil behaves as Newtonian and non-Newtonian. It is observed from Fig. 9 that for Newtonian behavior of oil, the magnitude of total pressure is low as compared to non-Newtonian behavior and lies in the range of 337 Pa to 450 Pa. Fig. 9 depicts that total pressure of mixture increases with the increase in the flow behavior index. For n = 0.7522 the total pressure lies in the range of 5534 pa to 5862.91 pa. For n = 0.8546 the total pressure lies in the range of 8832 Pa to 9008 Pa and for n = 0.9573 the total pressure lies in the range of 12755 Pa to 13182 Pa. The maximum total pressure in case of n = 0.9573, n = 0.8546 and 0.7522 are found to be higher than the maximum total pressure in case of stratified flow pattern by a factor of 29.29, 20.01 and 13.02 respectively. All the pressure variation curves are gradual and maxima appears in the region where dispersion takes place.

Table VI shows the pressure gradient along the length of the channel at different flow behavior index. As shown in the table the pressure gradient is strongly dependent on the nature

of fluid i.e. whether Newtonian or non-Newtonian. This is because the nature of the fluid plays a significant role in determining the flow pattern which has already been depicted and pressure gradient varies with flow pattern. There is a drastic change in the pressure gradient when the fluid changes its behavior from Newtonian to non-Newtonian and also when the flow behavior index is changed. As can be seen from the table the pressure gradient is very low in case of stratified flow pattern as compared to dispersed flow pattern for the same operating conditions. Also the pressure gradient is a strong function of flow behavior index. With the increase in flow behavior index, the pressure gradient along the length of the channel increases provided that the other parameters remain constant. This is because with the increase in flow behavior index the dispersion of phases increases which causes more pressure drop due to increase in friction in the flow.

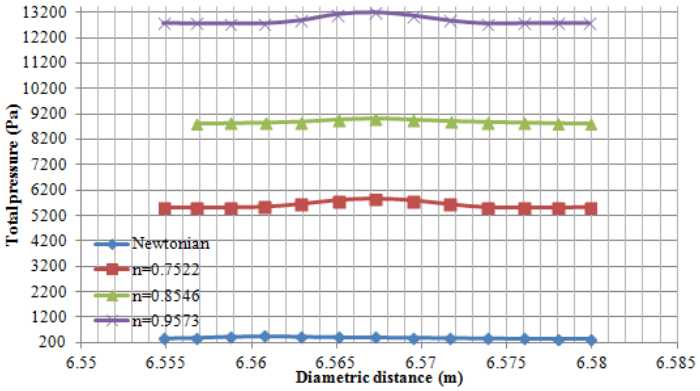

Fig. 9 Diametric distribution of total pressure at different flow behavior index

TABLE VI
PRESSURE GRADIENT DATA FOR THE CASE

S. N.	P_1 (pa)	P_2 (pa)	$-\partial P/\partial x$ (pa/m)
Newtonian	2117.602	61.505	287.164
n = 0.7522	25524.504	70.805458	3554.985
n = 0.8546	38381.195	78.644	5349.491
n = 0.9573	57369.699	65.378	8003.4

V. CONCLUSIONS

The attempts have been made to investigate one of the commonly found flow patterns in petroleum industries known as the stratified flow pattern. The simulations have been done for oil-water two phase flow in a rectangular 2D channel in unsteady mode. The interface between oil and water has been successfully captured using CLSVOF technique which has been proved to be better than volume of fluid method and level set techniques individually. All results have been obtained only after attainment of steady state. The simulation has been validated with the experimental data of Elseth [3] for stratified flow pattern and satisfactory agreement is obtained. The case has been investigated to understand some of the characteristics of stratified flow pattern. In each case, the diametric variation of volume fraction, mixture velocity, total pressure and pressure drop have been studied. Here oil has been assumed to behave as a non-Newtonian fluid and assumed to follow power law model. Three different values of the flow behavior index have been investigated. Interestingly instead of stratified flow, pattern disperse flow pattern is obtained for all values of flow behavior index. Total pressure of the mixture is found to be the most severely affected parameter due to this change in flow pattern. Magnitude of the maximum pressure is found to be almost 20 to 30 times higher than the pressure when oil is considered Newtonian. Pressure gradient is found to increase with increase in flow behavior index. Non-Newtonian behavior of oil is found to increase the pressure gradient in the flow by several orders of magnitude which results as increase in pumping power requirement. The results obtained could be useful in the design of transportation pipeline in oil industries.

ACKNOWLEDGEMENT

Authors heartily acknowledge National institute of Technology, Raipur for providing resources for this research article.

NOMENCLATURE

Symbols

k = Thermal conductivity of fluid (W/m-k)
C_p = Specific heat of fluid (J/kg-K)
K = Flow consistency index
n = flow behavior index
P = Pressure (Pa)
T = Temperature (k)
$\dot{m}$ = mass flux ($Kg\text{-}s^{-1}/m^2$)
r = Volume fraction
V = Mixture velocity (m/s)
V_o = Superficial velocity of oil (m/s)
V_w = Superficial velocity of water (m/s)
B = Body force per unit volume
x = space coordinate
t = time (s)
h_{12} = latent heat of phase change (J/kg)
$\hat{n}(\Phi)$ = unit vector normal to interface.
S_ϵ = smoothed sign function
$\Delta X\, \Delta Y$ = size of control volume in x and y directions
H = Heaviside function/Unit step function

∂P/∂x = pressure gradient (Pa/m)

Greek letters

ρ = Density of fluid

μ = Viscosity of fluid

σ = Surface tension coefficient

α = contact angle

τ = shear stress

ϕ = Level set function

δ = Dirac delta function

Γ = interface

θ = inlet to wall temperature ratio

€ = Half of the thickness of interface

Subscripts

m = mean

1= phase 1

2 = phase 2

Superscript

K= fluid index

REFERENCES

[1] S. Das, V. H. Gada, and A. Sharma, "Analytical and Level set method-based numerical study for two phase stratified flow in a pipe", *Numerical Heat Transfer, Part A,* 2015, vol. 67, pp.1253–1281.

[2] V. H. Gada, D. Datta, and A. Sharma, "Analytical and Level-Set method-based numerical study for two-phase stratified flow in a plane channel and a square duct", *Numerical Heat Transfer, Part A: Applications: An International Journal of Computation and Methodology,* 2011, vol.60:4, pp. 347-380.

[3] G. Elseth, "An experimental study of oil-water flow in horizontal pipes", *The Norwegian University of Science and Technology (NTNU) for the degree of Dr. Ing, 2001.*

[4] V. H. Gada, and A. Sharma, "Analytical and level-set method based numerical study on oil–water smooth/wavy stratified-flow in an inclined plane-channel", *International journal of Multiphase flow,* 2012, vol. 38:1, pp. 99-117.

[5] V. H. Gada, and A. Sharma, "On a novel dual grid Level Set method for two phase flow simulation", *Numerical heat Transfer part-B Fundamentals*, 2011, vol. 59:1, pp. 26-57.

[6] V. H. Gada, and A. Sharma, "On derivation and physical interpretation of Level set-Based equation for two phase flow simulation", *Numerical heat Transfer part-B Fundamentals*, 2009, vol. 56:4, pp.307-322.

[7] A. Goldstein, A. Ullmann, and N. Brauner, "Characteristics of stratified laminar flows in inclined pipes", *International Journal of Multiphase Flow,* 2015, vol.75, pp.267–287.

[8] S. Pandey, A. Gupta, D. Chakrabarti, G. Das, and S. Ray, "Liquid–liquid two phase flow through a horizontal T-junction", *Chemical Engineering Research and Design,* 2006, vol. 84 (A10), pp. 895–904.

[9] O. M. H. Rodriguez, and L.S. Baldani, "Prediction of pressure gradient and holdup in wavy stratified liquid–liquid inclined pipe flow", *Journal of Petroleum Science and Engineering,* 2012, vol. 96-97, pp. 140–151.